Published in final edited form as:
Hum Pathol. 2012 June ; 43(6): 790–800. doi:10.1016/j.humpath.2011.07.007.

Co-staining for Keratins 8/18 plus Ubiquitin Improves Detection of Hepatocyte Injury in Nonalcoholic Fatty Liver Disease

Cynthia D Guy[1], **Ayako Suzuki**[2], **James L Burchette**[1], **Elizabeth M Brunt**[3], **Manal F Abdelmalek**[2], **Diana Cardona**[1], **Shannon J McCall**[1], **Aynur Ünalp**[4], **Patricia Belt**[4], **Linda D Ferrell**[5], and **Anna Mae Diehl**[2] **for the Nonalcoholic Steatohepatitis Clinical Research Network**

[1]Department of Pathology, Duke University Medical Center, Durham, NC

[2]Division of Gastroenterology, Duke University Medical Center, Durham, NC

[3]Department of Pathology and Immunology, Washington University School of Medicine, Saint Louis, MO

[4]NASH CRN Data Coordinating Center, Johns Hopkins Bloomberg School of Public Health, Baltimore, MD

[5]Department of Pathology, University of California at San Francisco, San Francisco, CA

Abstract

Nonalcoholic fatty liver disease (NAFLD) is a global health dilemma. The gold standard for diagnosis is liver biopsy. Ballooned hepatocytes (BH) are histologic manifestations of hepatocellular injury and are characteristic features of steatohepatitis (SH), the more severe form of NAFLD. Definitive histologic identification of BH on routine stains, however, can be difficult. Immunohistochemical (IHC) evidence for loss of the normal hepatocytic keratins 8/18 (K8/18) can serve as an objective marker of BH. We sought to explore the utility of a K8/18 plus ubiquitin (Ub) double IHC stain for the histologic evaluation of adult NAFLD. Double IHC staining for

Corresponding author: Anna Mae Diehl, MD, Chief Division of Gastroenterology, Duke University School of Medicine, Snyderman Building (GSRB-1), 595 LaSalle Street, Suite 1073, Durham, NC27710, Phone: 919-684-2616, Fax 919-684-8857, diehl004@mc.duke.edu.

Author Conduct

Cynthia D Guy, MD: Generation of research concept and design, acquisition of data, data analysis and interpretation, and drafting, review, revision and approval of final manuscript.
Ayako Suzuki, MD, PhD: Data analysis, data interpretation, drafting and revision of manuscript.
James L Burchette, HT: Performed immunohistochemical staining, revision of manuscript.
Elizabeth M Brunt, MD: Generation of research concept and design, interpretation of data, review, revision and final approval of published manuscript
Manal F. Abdelmalek, MD, MPH: Participated in patient sample collection, drafting of research proposal, data interpretation, and revision of manuscript.
Diana Cardona, MD: Generation of data and data analysis, interpretation of results, review and revision of manuscript.
Shannon J. McCall, MD: Data analysis, interpretation of results, review and revision of manuscript.
Aynur Ünlap, MD, PhD: Generation of research design, interpretation of results, review and revision of manuscript. Patricia Belt, BS: Data coordination for the Nonalcoholic Steatohepatitis Clinical Research Network Pathology Committee, data acquisition, review and revision of manuscript.
Linda D. Ferrell, MD: Generation of research concept and design, review and revision and final approval of published manuscript.
Anna Mae Diehl, MD: Participated in patient sample collection, provided substantialcontributions to conception and design, interpretation of data, critical revision of the manuscript for important intellectual content, final approval for the published manuscript.

K8/18 and Ub was analyzed using 40 adult human NAFLD core liver biopsies. Ballooned hepatocytes lack K8/18 staining (KBH) as previously shown by others, but normal size hepatocytes with keratin loss (KH) are approximately five times greater in number than KBH. KBH, KH, and Ub deposits show a zonal distribution, are positively associated with each other, and are frequently found adjacent to or intermixed with fibrous matrix. All three lesions correlate with fibrosis stage and the H&E diagnosis of SH (all p values < 0.05). Compared to H&E staining, IHC staining improves the receiver operating characteristics curve for advanced fibrosis (0.77 vs. 0.83, 0.89, and 0.89 for KBH, KH, and Ub, respectively) because IHC is more sensitive and specific for fibrogenic hepatocellular injury than H&E staining. K8/18+Ub double IHC stain improves detection of hepatocyte injury in NAFLD. Thus, it may help differentiate NASH from NAFL.

Key words

Nonalcoholic steatohepatitis; ballooned hepatocytes; immunohistochemistry; endoplasmic reticulum stress; intermediate filaments; insulin resistance

Introduction

Nonalcoholic fatty liver disease (NAFLD) is comprised of two major histologic subtypes: nonalcoholic fatty liver (NAFL) and nonalcoholic steatohepatitis (NASH). Lipid accumulates within hepatocytes in both NAFL and NASH. The two entities differ, however, with regard to the prevalence and severity of hepatocyte injury and death (1). NASH is a more severe form of liver injury than NAFL and consequently, has a significantly greater likelihood of eventual cirrhosis and hepatocellular carcinoma (HCC) (2–6). Because the prognosis of NAFL and NASH are quite different, accurate diagnosis is important so that patients may be offered appropriate follow-up and treatment.

At present, histologic diagnosis is the gold standard for distinguishing NASH from NAFL (1, 7, 8). Pathologists review hematoxylin and eosin stained (H&E) liver biopsies for features indicative of ongoing hepatocyte injury. The latter include apoptotic bodies, inflammatory cell infiltration, and hepatocytes with aberrant morphology, such as cellular ballooning and accumulation of ubiquitinated cytokeratins (called Mallory-Denk bodies) (9). Because the diagnosis of NASH rests upon histologic evidence of hepatocyte injury, hepatocellular ballooning is one of the major diagnostic criteria for NASH. However, such ballooned hepatocytes (BH) can sometimes be difficult to appreciate on standard H&E-stained sections. A recent study by Professor Denk's group suggested immunohistochemical (IHC)staining for ubiquitin (Ub) and keratins 8 and 18 (K8/18) facilitates identification of BH, which are typically Ub+ but K8/18 negative (10). These staining characteristics are consistent with experimental data which demonstrate that pathways that normally mediate turnover of intracellular proteins (e.g., ubiquitination and proteasomal degradation) become disrupted in NASH, leading to endoplasmic reticulum (ER) stress that contributes to hepatocyte injury and increases the risk of fibrosis (11). Extension of this logic suggests that BH may be the extreme morphologic manifestations of dysfunctional protein turnover, and that improved methods to demonstrate ubiquitinated proteins and loss of K8/18 would improve sensitivity and/or specificity for detecting hepatocyte injury, and thereby diagnosing NASH. Improved ability to distinguish NASH from NAFL, in turn, is predicted to increase the accuracy of predicting risk for subsequent liver fibrosis.

In this study we performed double IHC staining for K8/18 and ubiquitin on a relatively large group of adult liver biopsy samples from the Nonalcoholic Steatohepatitis Clinical Research Network (NASH CRN) Database Study (12). All of the biopsies had been reviewed

previously by the NASH CRN Pathology Committee. During that process various histologic features were assigned scores according to NASH CRN criteria (7, 13) and each case was given a final diagnosis of definite NASH, definitely not NASH or suspicious for NASH based upon the group's consensus. The main objective of the current study was to determine if K8/18 plus Ub IHC staining improved detection of BH. Secondary aims were to characterize the relationship between loss of K8/18 staining, Ub accumulation, and other histologic features of liver damage, particularly fibrosis. We also examined correlations between the new markers of disrupted protein turnover and previously-identified clinical predictors of fibrosis progression, such as age, body mass index (BMI), and insulin resistance. Our results confirm that IHC staining improves detection of BH and support the concept that BH are the extreme manifestation of a more widespread defect in protein turnover, the severity of which strongly correlates with both the level of insulin resistance and fibrosis stage. The data also demonstrate that IHC staining reduces ambiguity in NAFLD diagnosis, thereby facilitating more accurate classification of NAFLD cases as either NAFL or NASH.

Materials and Methods

Study population and slide selection criteria

We evaluated one unstained section from 40 liver biopsies of clinically and histologically well-characterized adult NAFLD patients enrolled in the NASH CRN Database Study. Detailed description of the study design and operational structure of the NASH CRN and its associated clinical trials has been reported (12). All available liver biopsies from the enrolled patients were stained with H&E and Masson trichrome, and reviewed and scored centrally by the NASH CRN Pathology Committee according to a validated scoring system (7). Briefly, consensus scoring is performed by the NASH CRN Pathology Committee to establish: steatosis grade (0, <5% steatosis; 1, 5–33% steatosis; 2, 34–66% steatosis; and 3, >66% steatosis), steatosis location (zone 3, zone 1, azonal and panacinar), degree of lobular inflammation per 200× HPF (0, none; 1, <2 foci; 2, 2–4 foci; 3, >4 foci), degree of ballooning (0, none; 1, few; 2, many), the presence of Mallory-Denk bodies (0, absent/rare; 1, many), the diagnosis of steatohepatitis (0, not SH; 1, suspicious for SH; 2 definite SH) and the degree of fibrosis (0, no fibrosis; 1, modified Brunt stage 1; 2, Brunt stage 2; 3, bridging; 4, cirrhosis).

Cases for the current study were selected from the NASH CRN Database Study repository to generate a representative cohort that reflected the spectrum of liver injury and fibrosis in NAFLD. Briefly, the NASH CRN Database Study is comprised of a total of 1,044 enrolled patients. Of those, 864 had a baseline liver biopsy available for review by the NASH CRN Pathology Committee. Only 459 of those had biopsies that were > 15 mm long, 355 of those contained steatosis of at least 5% (which is considered the minimal amount of steatosis to fulfill the definition of NAFLD), and 209 of those 355 biopsies had been obtained within 6 months of registration into the study.

From that available pool of 209 cases, the NASH CRN Data Coordinating Center provided us with a cohort of 40 cases based on the Pathology Committee scoring results for the degree of ballooning and the diagnostic categorization (not SH, suspicious for SH, or definite SH). In order to achieve a desired mix of cases that represent the full spectrum of NAFLD, the following cases were selected: ballooning grade 0 (no ballooning) 50%, ballooning grade 1 (few ballooned hepatocytes) 20%, ballooning grade 2 (many ballooned hepatocytes) 30%, not diagnostic of NASH (40%), suspicious for NASH (20%), and definite NASH (40%). One slide from each of these cases was forwarded to Duke for IHC staining; immunohistochemistry was performed and those data were quantified before the results of

the NASH CRN Pathology Committee scoring and other clinical/laboratory data were supplied.

The NASH CRN studies have been approved by the Institutional Review Boards at each participating center. This study has been approved by NASH CRN Ancillary Studies Committee and the NASH CRN Publications and Presentations Committee and was conducted using only deidentified data provided from NASH CRN and did not directly involve human subjects.

Keratin 8/18 plus Ubiquitin Immunohistochemical Stain

One unstained section from the forty formalin-fixed liver biopsies was used for IHC staining. Briefly, an antibody cocktail of brown chromagen-tagged mouse monoclonal keratin 8 and 18 (K8/18) (Leica Microsystems, Bannockburn IL, RTU reagent diluted 1:2) and a red chromagen-tagged ubiquitin rabbit polyclonal (Dako USA, Carpinteria CA, diluted 1:500) was prepared and applied to the tissue sections.

Details of the IHC staining protocol are as follows. One 5 micron thick unstained section from each of the forty formalin-fixed core liver biopsies was used for IHC staining. After removal of paraffin with xylene and clearing with alcohol, the slides were placed in hydrogen peroxide and methanol to quench endogenous peroxidase activity. The sections were hydrated and washed with deionized water. Pretreatment of the tissue sections was performed using proteolytic enzyme pepsin (0.25%, pH 2.0) for 15 minutes at 37° C. The slides were rinsed with deionized water and placed in Tris buffered saline procedural buffer (TBS) pH 7.5. An antibody cocktail of mouse monoclonal keratin 8 and 18 (K8/18) (Leica Microsystems, Bannockburn IL, RTU reagent diluted 1:2) and ubiquitin rabbit polyclonal (Dako USA, Carpinteria CA, diluted 1:500) was prepared. Tissue sections were incubated for 1 hour at room temperature. A negative control consisting of a cocktail of mouse IgG and rabbit IgG was run in parallel with the primary antibody. Following incubation with primary antibody, the slides were rinsed and washed with TBS. Mach 2, kit number 2 (Biocare Medical, Concord CA) containing a cocktail of horseradish peroxidase conjugated anti-mouse and alkaline phosphatase conjugated anti-rabbit was used to label the bound primary antibodies. Diaminobenzidine (DAB) was used to visualize the bound CK8/18 antibody. Following the application of DAB, the slides were washed with deionized water and Vulcan Fast Red (Biocare Medical) was applied to the tissue sections to demonstrate the bound ubiquitin antibody. Hematoxylin counter stain was applied, followed by rapid dehydration with alcohol, clearing with xylene and permanent cover slipping.

Morphologic assessment of liver biopsies

Every 20× objective high power field (HPF, magnification = 200×) of each biopsy was evaluated for: the number of hepatocytes enlarged to at least 1.5 to 2 times the size of normal and lacking K8/18 staining (KBH), the number of KBH positive for Ub, the number of normal size hepatocytes lacking K8/18 staining (KH), the number of KHs positive for ubiquitin, and the total number of ubiquitin particles. The counted ubiquitin aggregates were large and the width tended to be at least half the size of the hepatocyte nucleus. Ubiquitin was counted whether it was intracellular or extracellular. The acinar location of each lesion was recorded. Whether the lesions were located adjacent to fibrosis was recorded; fibrosis was defined as extracellular, keratin negative, spindled cell matrix. To standardize for the differences in biopsy sample length, the number of counted lesions was expressed as a normalized number per 10 HPFs and analyzed as described below.

Clinical and histologic data of the cohort

As described above, all 40 cases had been previously reviewed and scored by the NASH CRN Pathology Committee using the H&E and trichrome stained slides. Those histologic scoresand the following clinical information and laboratory data were obtained from the NASH CRN Data Coordinating Center: age, gender, BMI (kg/m^2), presence of diabetes mellitus, alanine aminotransferase (ALT), aspartate aminotransferase (AST), and homeostasis model assessment–insulin resistance [HOMA-IR].,

Statistical analysis

Clinical characteristics are reported as the mean ± the SD or the median with 25^{th}–75^{th} percentiles for continuous variables, or as a proportion with a condition for dichotomized variables. We first described numbers, proportions with 95% confidence interval (95%CI), zonal distribution, and physical relationship to fibrous matrix deposition of the three IHC lesions (i.e., KBH, ubiquitin aggregates, and KH). The proportions were analyzed using the Chi-square test. In single sample Chi-square tests, the proportions were compared with hypothetical probabilities of 50% for two-category comparisons or 33.3% for three-category comparisons. To assess correlations among the IHC lesions, we performed linear regression analysis.

To assess the relationships of the IHC lesions with the histologic scores read by the NASH CRN Pathology Committee, we performed the Kruskal-Wallis test. Also, we performed the Chi-square test after categorizing the IHC lesions into three groups: none, few (<10), and many (≥10) per 10 HPFs. To compare the performance of the IHC lesions versus the H&E diagnosis of SH in predicting advanced fibrosis, we performed logistic regression analysis with ROC curve analysis using advanced fibrosis (stage 3 and 4) as a dependent variable.

To assess relationships of the IHC lesions with known clinical risk factors of advanced NAFLD (i.e., age, BMI, HOMA-IR, and presence of diabetes mellitus), we performed the Kruskal-Wallis test using categorized variables of the IHC lesions (none, few and many) as independent variables. The one case in which clinical and laboratory data were not obtained within 6 months from the date of biopsy was excluded from the analysis.

For analyses, we used JMP statistical software version 7.0(SAS Institute Inc, Cary, NC) and considered differences statistically significant when the p-values were less than 0.05. All p values presented are two-sided and have not been adjusted for multiple comparisons.

Analysis of interobserver variance and the practical utility of IHC compared to H&E

As a separate analysis, we performed a pilot study to access the practical application of using this IHC stain, and to compare the interobserver variance between the evaluations of degree of ballooning, the diagnosis of SH, degree of fibrosis and the IHC evaluation of hepatocellular injury. Unfortunately, matching H&E and trichrome stained slides from only 27 of the 40 patients in the cohort were available from the NASH CRN storage facility. Two of our localexperienced hepatopathologists (CG and DC) were asked to read the 27 pairs of slides and score 1) ballooning (none, few, or many), 2) steatohepatitis (no, suspicious, or definite), and 3) stage. At a separate time, they were asked to read the corresponding 27 IHC stained slides to evaluate for any of the three lesions (i.e., KBH, ubiquitin deposits, or KH) as seen using the scanning 10× objective (100× magnification) and score them as no, rare (</= 4), or many (>4) foci of injury. The results from the two pathologists were tabulated to calculate observed agreement (% and 95% CI) and kappa scores.

Results

Characteristics of the cohort

The mean age and BMI were 50 ± 11 years old and 35.4 ± 6.5 kg/m^2, respectively; women comprised 57.5% of the cohort. Median values and interquartile ranges of serum ALT, AST, and HOMA-IR were 54 U/L [37, 75], 43 U/L [28, 53], and 3.9 [2.5, 7.5]. The distributions of histologic scores are summarized in Table 1. Overall, 32.5% of the cases had a nonalcoholic fatty liver disease activity score (NAS) of ≥ 5, 40.0% haddefinite steatohepatitis, and 25% had advanced fibrosis (17.5% bridging fibrosis, 7.5% cirrhosis).

Keratin 8/18 plus ubiquitin immunohistochemistry data

Since K8/18 is the major cytoskeletal filament in normal hepatocytes, dark and homogenous staining is characteristic. The K8/18 staining quality was flawless in 24 of the 40 cases, and thus every 20× objective high power field (HPF) was evaluated on each of those sections. In 14 cases the keratin staining was somewhat lighter and patchy, so only HPFs with sufficient staining quality were evaluated (Figure 1). The mediannumber of HPFs/section evaluated in these 14 cases was19 [with interquartile ranges of 7 and 23]. The median proportion of HPF/section evaluated in these 14 cases was 76% [with interquartile ranges of 25 – 95%]. In 2 cases keratin staining was diffusely suboptimal, precluding analysis of KH. Overall, keratin staining was analyzed in more than 10 HPF/section in 85% of the cases. Cases with poorly stained sections were distributed across the full spectrum of NAFLD severity. The Ub staining was sufficient for analysis in all cases.

A total 974 HPFs were evaluated. The average number of HPFs read per case was 24.4 ± 7.4. A total of 95 KBH, 487 KH, and 1437 Ub aggregates were detected. A wide range of KBH (0–21), KH (0–45), and Ub (0–147/) per 10 HPFs were observed among individual cases, in keeping with the heterogeneous nature of our cohort. Overall, 29.7%, 37.1% and 56.4% of the cases were positive for KBH, KH, and Ub.

KBH, KH and Ub were zonally distributed (zone 3 > zone 1 > zone 2; $p < 0.0001$) (Table 2). The majority (about two thirds) of such lesions were located in zone 3, while most of the remaining KBH, KH and Ub particles were located in zone 1. Linear regression analyses demonstrated that the numbers of KBH, KH, and Ub were significantly correlated with each other in individual cases ($R^2 = 0.84$, $p<0.0001$ for Ub and KH; 0.58, $p<0.0001$ for KH and KBH; 0.48, $p<0.0001$ for Ub and KBH). All cases lacking Ub were also negative for KBH and KH, while a few cases negative for KBH or KH contained Ub. Overall, 70% of the KBH and 88% of the KH were positive for Ub, revealing that most cells that lacked K8/18 staining contained aggregates of ubiquitinated proteins, even if they were not overtly ballooned.

The zonality and physical relationship of KBH, KH and Ub to extracellular matrix is summarized in Table 3. The large majority of KBH, Ub, and KH were observed adjacent to fibrosis: 85% of KBH, 94% of Ub, and 90% of KH were localized near fibrosis. Keratin-negative hepatocytes that were also Ub-positive localized adjacent to fibrosis more often than KH that lacked Ub (91.0% vs. 81.5%; Chi-square test, $p<0.02$). KBH were typically associated with fibrosis, whether or not they contained Ub aggregates.

Comparisons between H&E staining and IHC

Representative photographs of ballooned hepatocytes (with H&E and trichrome staining), KBH, KH, and Ub (with IHC staining) are shown in Figure 1. The IHC stained sections revealed hepatocyte injury (as evidenced by KBH, KH, and/or Ub) that was sometimes not easily appreciated on the H&E stained sections.

An association between azonally-distributed steatosis and higher values of KBH, Ub deposits, and KH emerged when sections were analyzed after IHC (Table 4). The numbers of KBH, Ub, and KH generally correlated with the severity of ballooning, the presence of Mallory-Denk bodies, the diagnosis of steatohepatitis, and fibrosis stage. However, the more sensitive detection of hepatocyte injury by IHC staining would have impacted histologic grading in individual cases (Figure 2). For example, one of the 18 cases (6%) in which no ballooned hepatocytes were identified on H&E staining (ballooning grade 0) showed evident KBH, while 6 of 8 cases (75%) judged to have ballooning grade 1 (few ballooned hepatocytes) and 4 of 12 cases (33%) in which ballooning was grade 2 (many ballooned hepatocytes) by H&E staining did not show any KBH. Comparison of IHC evidence of Ub with Mallory-Denk bodies on H&E staining also revealed some important scoring differences. Eight of 31 cases (26%) with no Mallory-Denk bodies on H&E (grade 0) demonstrated Ub.

IHC staining was particularly useful for evaluating the degree of hepatocellular injury in cases that were classified as suspicious for SH. Five of the 7 cases in this category (71%) showed no KBH, 5 of 8 (62%) showed no Ub, and 4 of 6 (67%) showed no KH. Thus the absence of IHC evidence for significant hepatocellular injury was noted in at least two-thirds of the cases in which the NAFLD classification had been equivocal by routine staining. Similarly, IHC would have refined categorization of cases that had been classified as definite SH. Seven of 16 cases with an H&E-based diagnosis of “definite SH” (44%) showed no KBH, 2 of 16 (12%) showed no Ub, and 4 of 15 (27%) showed no KH. Thus, the most conservative interpretation of the IHC data indicates that about one out of 10 cases that were presumed to have definite NASH based on evaluation of routinely stained liver sections, did not show sufficient evidence of hepatocellular injury on IHC evaluation.

The concept that IHC analysis was more accurate for demonstrating hepatocellular injury compared to analysis of conventional staining alone was further supported by logistic regression with receiver operating characteristics (ROC) curve analyses for co-existent advanced fibrosis, an accepted outcome of chronic liver injury. The categorized variables of KBH, Ub, and KH each consistently yielded a higher area under the receiver operating characteristics (AUROC) curve (0.89, 0.89, and 0.83, respectively) than the ballooning grades from H&E-stained sections (0.77).

Inter-observer variance of IHC versus H&E

To determine whether IHC improved inter-observer agreement about the presence of absence of hepatocellular injury, two experienced liver pathologists from our institution independently reviewed and scored the 27 available NAFLD sections stained with H&E and trichrome, and separately reviewed and scored the corresponding 27 IHC stained sections. Interobserver variance for detecting hepatocellular injury, identifying BH, diagnosing SH, and staging liver fibrosis was then calculated. Based upon analysis of H&E and trichrome-stained sections, the two observers were in agreement about two thirds of the time regarding the severity of hepatocyte ballooning (66.7%), presence or absence of SH (66.7%) and fibrosis stage (63.0%). IHC improved agreement about the presence or absence of hepatocellular injury (requisite to establish a diagnosis of NASH) to 77.8%. The fact that IHC staining improved consensus about the severity of hepatocyte injury was further supported by the calculated kappa scores; the kappa score was 0.49 for the H&E-based diagnosis of SH, versus 0.61 when evaluation of injury was based on the reading of IHC stained sections.

Relationships of KBH, Ub deposits, and KH with clinical risk factors of hepatic fibrosis

Univariate analysis did not demonstrate significant associations between age, BMI, and the presence of diabetes mellitus with numbers of KBH, Ub, or KH. HOMA-IR, however, was positively associated with KBH and Ub (Kruskal-Wallis tests: p=0.02 and p=0.07, respectively). NAFLD patients whose biopsies demonstrated KBH or Ub had higher HOMA-IR values than patients whose biopsies lacked these lesions (Figure 3).

Discussion

The most important finding of our study is that IHC staining for K8/18 and Ub facilitates the detection of injured hepatocytes in fatty livers. Our data confirm another recent report which demonstrated that ballooned hepatocytes, a classical hallmark of SH, generally lack K8/18 staining and often harbor aggregates of ubiquitinated proteins (10). These characteristics permit ballooned hepatocytes to be easily recognized on IHC-stained liver sections, whereas they can be difficult to appreciate with routine H&E staining. In addition, we show that this IHC staining technique is useful for revealing other hepatocytes that are not yet ballooned, but which also manifest loss of the typical hepatocyte keratins and/or contain Ub aggregates. These non-ballooned, but dysmorphic, hepatocytes typically localize near each other and in close proximity to KBH in zone 3 or zone 1, suggesting that all of these aberrant morphologies reflect similar types of cellular stress. Given that ubiquitinated K8 and K18 are the major constituents of Mallory-Denk bodies (14), the fact that Mallory body formation has been mechanistically linked with defective protein turnover and ER stress (15, 16), and other evidence that ballooned hepatocytes exhibit markers of the ER stress response (17), ER stress is the most likely culprit for the loss of K8/18 and accumulation of ubiquitinated proteins in non-ballooned hepatocytes in patients with NAFLD. Further support for this concept derives from our observation that the numbers of KBH, KH, and Ub in NAFLD patients increase in parallel with HOMA-IR scores, because a cause-effect relationship between ER stress and insulin resistance has already been established. For example, genetic manipulations that provoke ER stress were proven to induce insulin resistance in mice (18), while interventions that reduced ER stress improved insulin resistance in experimental animals (18–20). The unfolded protein response and ER stress have also been linked to the pathogenesis of steatosis (21), and our data demonstrate a strong association between steatosis location and accumulation of KBH, KH, and Ub deposits. Hence, IHC is a more sensitive approach than standard H&E staining for revealing ongoing ER stress-related hepatocyte injury that is known to develop in the context of hepatic steatosis (11), and to promote further hepatic lipid accumulation and insulin resistance in this condition.

The improved accuracy of detecting injured hepatocytes with this IHC staining provides a more accurate classification of NAFLD cases as either NAFL or NASH. This is a critically important distinction because potentially fatal forms of chronic liver disease (cirrhosis or HCC) result much more commonly from NASH than NAFL (3–6). Indeed, our data show that IHC-based identification of hepatocyte injury (as demonstrated by accumulation of KBH, KH and/or Ub) provides a more reliable correlate of liver fibrosis than H&E based detection of hepatocyte injury. Moreover, the new staining approach clearly demonstrates the strong tendency for fibrosis to accumulate predominately in areas that are enriched with injured hepatocytes. These findings complement other lines of evidence which indicate that the level of liver cell death predicts fibrosis severity (22), while raising questions about the mechanisms involved. Keratin 8 and 18 are known to exert cytoprotective functions (14, 23–26). When normal turnover of these proteins is disturbed, aggregates of ubiquitinated K8/18 (MDBs) develop while cellular content of functional K8/18 proteins declines. The latter is predicted to make hepatocytes more vulnerable to injury. Because IHC staining reveals that viable KH typically localize near fibrous septae, it is conceivable that such cells may release

fibrogenic factors even before they die. Additional research will be needed to address this issue directly. Such work holds the potential for identifying novel therapeutic targets to prevent NAFLD-related fibrogenesis, as well as for development of noninvasive biomarkers to identify and track NASH patients who are at greatest risk for cirrhosis. Until the latter advances occur, however, IHC-related improvements in the accuracy of histologic classification of NAFLD will almost certainly impact design and interpretation of future therapeutic trails in the NAFLD field.

Acknowledgments

Funding: The Nonalcoholic Steatohepatitis Clinical Research Network (NASH CRN) is supported by the National Institute of Diabetes and Digestive and Kidney Diseases (NIDDK) (grants U01DK061718, U01DK061728, U01DK061731, U01DK061732, U01DK061734, U01DK061737, U01DK061738, U01DK061730, U01DK061713). Several clinical centers use support from General Clinical Research Centers or Clinical and Translational Science Awards in conduct of NASH CRN Studies (grants UL1RR024989, M01RR000750, M01RR00188, UL1RR02413101, M01RR000827, UL1RR02501401, M01RR000065, M01RR020359). Dr. Manal F. Abdelmalek is supported by a National Institute of Diabetes and Kidney Disease (NIDDK) K23 Career Development Award (K23-DK062116). Dr. Anna Mae Diehl is supported by a National Institute of Health Grant (RO1 DK077794).

Abbreviations

ALT	alanine aminotransferase
AST	aspartate aminotransferase
AUROC	area under the receiver operating characteristic curve
BH	ballooned hepatocytes
BMI	body mass index
DAB	diaminobenzidine
ER	endoplasmic reticulum
H&E	hematoxylin and eosin
HCC	hepatocellular carcinoma
IHC	immunohistochemical
HPF	high power field
K8/18	keratins 8 and 18
KBH	keratin negative ballooned hepatocytes
HOMA-IR	homeostatic model assessment of insulin resistance
KH	keratin negative (normal size) hepatocytes
MDB	Mallory-Denk bodies
NAFL	nonalcoholic fatty liver
NAFLD	nonalcoholic fatty liver disease
NAS	nonalcoholic steatohepatitis activity score
NASH CRN	Nonalcoholic Steatohepatitis Clinical Research Network
NPV	negative predictive value
PPV	positive predictive value

ROC	receiver operating characteristics
SH	steatohepatitis
TBS	Tris buffered saline
Ub	ubiquitin or ubiquitinated protein aggregates

REFERENCES

1. Matteoni CA, Younossi ZM, Gramlich T, Boparai N, Liu YC, McCullough AJ. Nonalcoholic fatty liver disease: a spectrum of clinical and pathological severity. Gastroenterology. 1999; 116:1413–1419. [PubMed: 10348825]
2. Sanyal AJ. AGA technical review on nonalcoholic fatty liver disease. Gastroenterology. 2002; 123:1705–1725. [PubMed: 12404245]
3. McCullough AJ. Update on nonalcoholic fatty liver disease. J Clin Gastroenterol. 2002; 34:255–262. [PubMed: 11873108]
4. Adams LA, Lindor KD. Nonalcoholic fatty liver disease. Ann Epidemiol. 2007; 17:863–869. [PubMed: 17728149]
5. Starley BQ, Calcagno CJ, Harrison SA. Nonalcoholic fatty liver disease and hepatocellular carcinoma: a weighty connection. Hepatology. 2010; 51:1820–1832. [PubMed: 20432259]
6. Soderberg C, Stal P, Askling J, et al. Decreased survival of subjects with elevated liver function tests during a 28-year follow-up. Hepatology. 51:595–602. [PubMed: 20014114]
7. Kleiner DE, Brunt EM, Van Natta M, et al. Design and validation of a histological scoring system for nonalcoholic fatty liver disease. Hepatology. 2005; 41:1313–1321. [PubMed: 15915461]
8. Brunt EM. Nonalcoholic steatohepatitis. Semin Liver Dis. 2004; 24:3–20. [PubMed: 15085483]
9. Zatloukal K, French SW, Stumptner C, et al. From Mallory to Mallory-Denk bodies: what, how and why? Exp Cell Res. 2007; 313:2033–2049. [PubMed: 17531973]
10. Lackner C, Gogg-Kamerer M, Zatloukal K, Sumptner C, Brunt EM, Denk H. Ballooned hepatocytes in steatohepatitis: the value of keratin immunohistochemistry for diagnosis. J Hepatol. 2008; 48:821–828. [PubMed: 18329127]
11. Puri P, Mirshahi F, Cheung O, et al. Activation and dysregulation of the unfolded protein response in nonalcoholic fatty liver disease. Gastroenterology. 2008; 134:568–576. [PubMed: 18082745]
12. Nonalcoholic steatohepatitis clinical research network. Hepatology. 2003; 37:244. [PubMed: 12540771]
13. Brunt EM. Nonalcoholic steatohepatitis (NASH): further expansion of this clinical entity? Liver. 1999; 19:263–264. [PubMed: 10459622]
14. Omary MB, Ku NO, Strnad P, Hanada S. Toward unraveling the complexity of simple epithelial keratins in human disease. J Clin Invest. 2009; 119:1794–1805. [PubMed: 19587454]
15. Harada M, Hanada S, Toivola DM, Ghori N, Omary MB. Autophagy activation by rapamycin eliminates mouse Mallory-Denk bodies and blocks their proteasomal inhibitor-mediated formation. Hepatology. 2008; 47:2026–2035. [PubMed: 18454506]
16. Strnad P, Tao GZ, So P, et al. “Toxic memory” via chaperone modification is a potential mechanism for rapid Mallory-Denk body reinduction. Hepatology. 2008; 48:931–942. [PubMed: 18697205]
17. Caldwell S, Ikura Y, Dias D, et al. Hepatocellular ballooning in NASH. J Heptatol. 2010; 53:719–723.
18. Ozcan U, Cao Q, Yilmaz E, et al. Endoplasmic reticulum stress links obesity, insulin action, and type 2 diabetes. Science. 2004; 306:457–461. [PubMed: 15486293]
19. Kammoun HL, Chabanon H, Hainault I, et al. GRP78 expression inhibits insulin and ER stress-induced SREBP-1c activation and reduces hepatic steatosis in mice. J Clin Invest. 2009; 119:1201–1215. [PubMed: 19363290]

20. Yoshiuchi K, Kaneto H, Matsuoka TA, et al. Pioglitazone reduces ER stress in the liver: direct monitoring of in vivo ER stress using ER stress-activated indicator transgenic mice. Endocr J. 2009; 56:1103–1111. [PubMed: 19789420]

21. Rutkowski DT, Wu J, Back SH, et al. UPR pathways combine to prevent hepatic steatosis caused by ER stress-mediated suppression of transcriptional master regulators. Dev Cell. 2008; 15:829–840. [PubMed: 19081072]

22. Feldstein AE, Canbay A, Angulo P, et al. Hepatocyte apoptosis and fas expression are prominent features of human nonalcoholic steatohepatitis. Gastroenterology. 2003; 125:437–443. [PubMed: 12891546]

23. Strnad P, Tao GZ, Zhou Q, et al. Keratin mutation predisposes to mouse liver fibrosis and unmasks differential effects of the carbon tetrachloride and thioacetamide models. Gastroenterology. 2008; 134:1169–1179. [PubMed: 18395095]

24. Moll R, Divo M, Langbein L. The human keratins: biology and pathology. Histochem Cell Biol. 2008; 129:705–733. [PubMed: 18461349]

25. Ku NO, Strnad P, Zhong BH, Tao GZ, Omary MB. Keratins let liver live: Mutations predispose to liver disease and crosslinking generates Mallory-Denk bodies. Hepatology. 2007; 46:1639–1649. [PubMed: 17969036]

26. Zatloukal K, Stumptner C, Lehner M, et al. Cytokeratin 8 protects from hepatotoxicity, and its ratio to cytokeratins 18 determines the ability of hepatocytes to form Mallory bodies. Am J Pathol. 2000; 156:1263–1274. [PubMed: 10751352]

Members of the Nonalcoholic Steatohepatitis Clinical Research Network

Clinical Centers

Case Western Reserve University Clinical Centers:

- **MetroHealth Medical Center, Cleveland, OH:** Arthur J. McCullough, MD; Patricia Brandt; Srinivasan Dasarathy, MD; Jaividhya Dasarathy, MD; Carol Hawkins, RN; Yao-Chang Liu, MD (2004–2009);
- **Cleveland Clinic Foundation, Cleveland, OH:** Arthur J. McCullough, MD; Srinivasan Dasarathy, MD; Mangesh Pagadala,MD; Ruth Sargent, LPN; Lisa Yerian, MD; Claudia Zein, MD

California Pacific Medical Center: Raphael Merriman, MD; Anthony Nguyen

Duke University Medical Center, Durham, NC: Manal F. Abdelmalek, MD, MPH; Stephanie Buie; Anna Mae Diehl, MD; Marcia Gottfried, MD (2004–2008); Cynthia D Guy, MD; Meryt Hanna; Paul Killenberg, MD (2004–2008); Samantha Kwan, MS (2006–2009); Yi-Ping Pan; Dawn Piercy, FNP; Melissa Smith

Indiana University School of Medicine, Indianapolis, IN: Elizabeth Byam, RN; Naga Chalasani, MD; Oscar W. Cummings, MD; Ann Klipsch, RN; Jean P. Molleston, MD; Linda Ragozzino, RN; Girish Subbarao, MD; Raj Vuppalanchi, MD

Johns Hopkins Hospital, Baltimore, MD: Michael Torbenson, MD

Saint Louis University, St Louis, MO: Joyce Hoffmann; Debra King, RN; Andrea Morris; Joan Siegner, RN; Susan Stewart, RN; Brent A. Neuschwander-Tetri, MD; Judy Thompson, RN

University of California San Diego, San Diego, CA: Cynthia E Behling, MD, PhD; Janis Durelle; Rohit Loomba, MD; Anya Morgan; Heather Patton, MD

University of California San Francisco, San Francisco, CA: Nathan M. Bass, MD, PhD; Linda D. Ferrell, MD; Mark Pabst; Philip Rosenthal, MD

University of Washington Medical Center, Seattle, WA: Matthew Yeh, MD, PhD

Virginia Commonwealth University, Richmond, VA: Sherry Boyett, RN, BSN; Melissa J. Contos, MD; Michael Fuchs, MD; Amy Jones; Velimir AC Luketic, MD; Puneet Puri, MD;Arun J. Sanyal, MD; Carol Sargeant, RN, BSN, MPH; Kimberly Noble;

Virginia Mason Medical Center1, Seattle, WA: Kris V. Kowdley, MD; Jody Mooney, MS; James Nelson, PhD; Sarah Ackermann; Cheryl Shaw, MPH; Vy Trinh; Chia Wang, MD

Washington University, St. Louis, MO: Elizabeth M. Brunt, MD

Resource Centers

National Cancer Institute, Bethesda, MD: David E. Kleiner, MD, PhD

National Institute of Diabetes and Digestive and Kidney Diseases, Bethesda, MD: Edward C. Doo, MD; Jay H. Hoofnagle, MD; Patricia R. Robuck, PhD, MPH (Project Scientist)

Johns Hopkins University, Bloomberg School of Public Health (Data Coordinating Center), Baltimore, MD: Patricia Belt, BS; Jeanne M. Clark, MD, MPH; Ryan Colvin, MPH; Michele Donithan, MHS; Mika Green, MA; Milana Isaacson, BS; Wana Kim, BS; Laura Miriel; Alice Sternberg, ScM; James Tonascia, PhD; Aynur Ünalp, MD, PhD; Mark Van Natta, MHS; Ivana Vaughn, MPH; Laura Wilson, ScM; Katherine Yates, ScM

[1]original grant with University of Washington

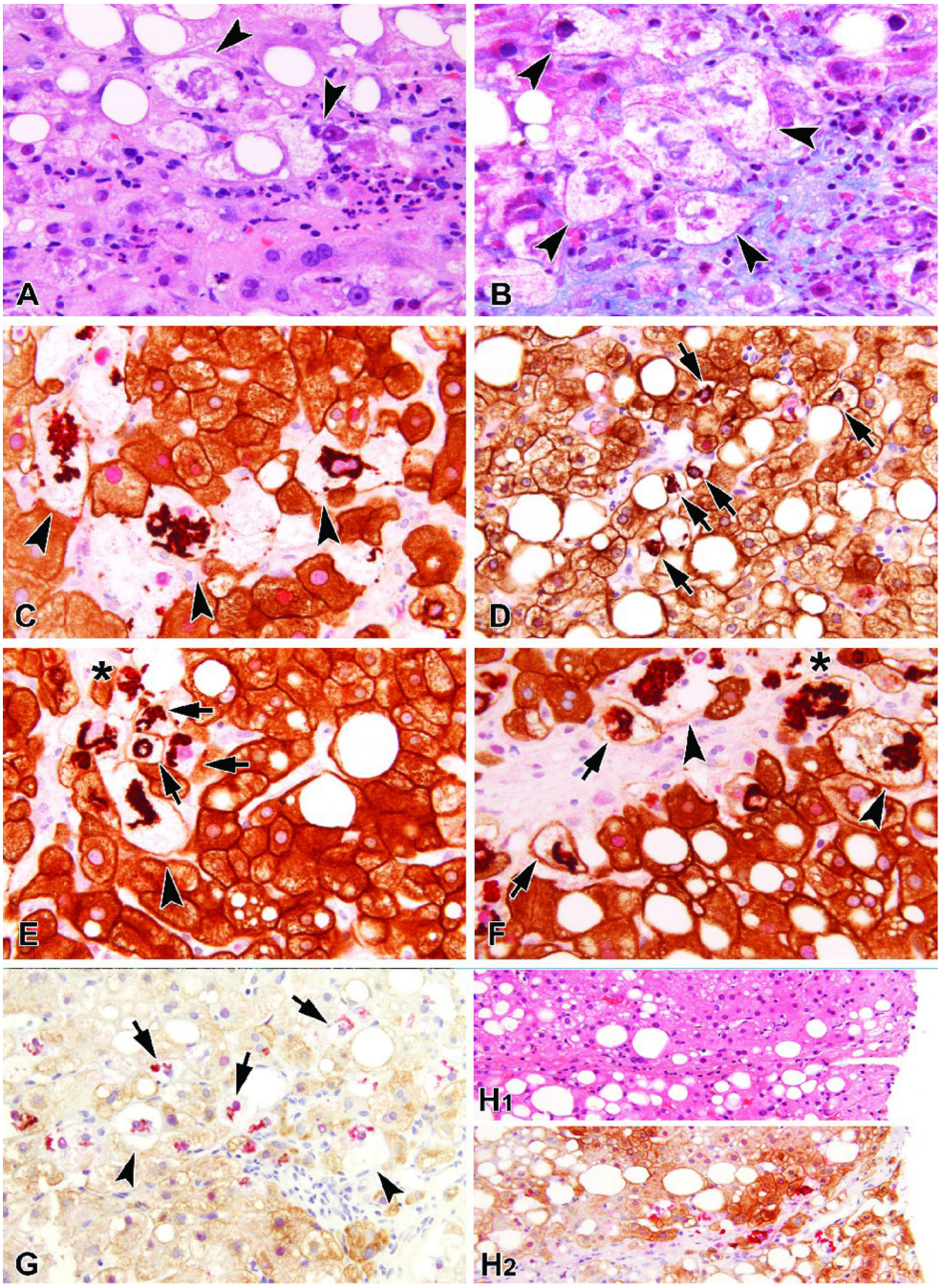

FIGURE 1.

H&E and IHC stained sections showing hepatocellular injury. (A) An H&E stained section shows easily identified enlarged, rounded, swollen-appearing ballooned hepatocytes (arrow heads) with cytoplasmic clearing and reticulation and perinuclear Mallory-Denk bodies. (B) A Masson trichrome stained section shows numerous ballooned hepatocytes (arrow heads) with associated fibrosis. (C) K8/18 plus ubiquitin double IHC stained section shows several enlarged keratin negative ballooned hepatocytes (KBH) (arrow heads). The red-chromagen tagged ubiquitin antibody highlights Mallory-Denk bodies. The adjacent normal size hepatocytes show the usual homogeneous cytoplasmic staining with the brown chromagen-tagged K8/18 antibody. (D) Many normal size hepatocytes show complete loss of K8/18

staining (KH) (arrows). These KH also contain Mallory-Denk bodies. (E and F) Typical examples of foci of hepatocellular injury as seen with the double IHC stain. KBH (arrow heads) and KH (arrows) are often co-localized and adjacent to or intermixed with fibrosis. Many ubiquitinated protein aggregates are perinuclear, however, extracellular ubiquitin deposits (asterisks) can often also be identified. (G) In some cases, K8/18 staining was faint and patchy, however, KBH (arrow heads) and KH (arrows) can still be identified. (H1–H2) H1shows an H&E stained section of a somewhat linear area of fibrosis in which ballooned hepatocytes are not detected. H2 shows the double IHC stained section of the same focus; hepatocytes with loss of keratin staining and ubiquitin deposits are easily seen.

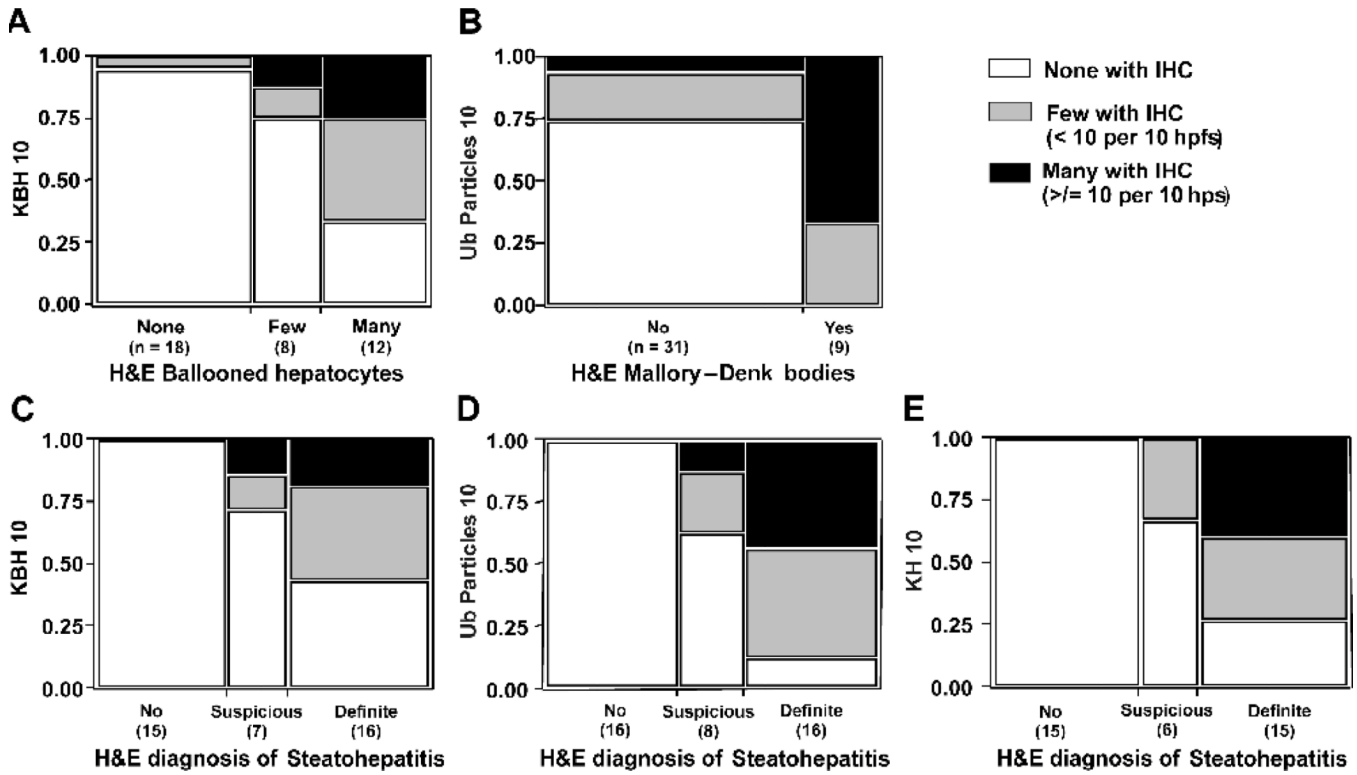

FIGURE 2.

Contingency plot analyses comparing H&E scoring parameters with IHC detection of hepatocellular injury. (A) The H&E scoring of ballooned hepatocytes is compared to the IHC analysis of KBH, (B) the H&E scoring of MDBs is compared to the IHC analysis of Ub deposits, (C) the H&E diagnosis of SH is compared to the IHC analysis of KBH, (D) the H&E diagnosis of SH is compared to the IHC analysis of Ub deposits, and (E) the H&E diagnosis of SH is compared to the IHC analysis of KH.

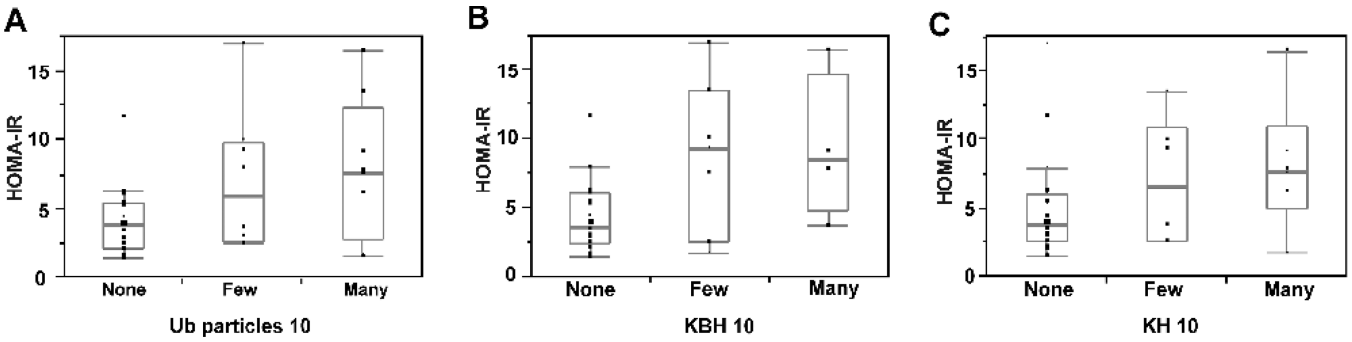

FIGURE 3.

Box plot graph with HOMA-IR (mg/dl*μU/ml) shown on the vertical axis and 'None' (0 per 10 HPFs), 'Few' (>0 and <10 per hpfs) and 'Many' (≥10 per hpfs) ubiquitin particles, KBH, and KH on the horizontal axis. The boxes represent the median (middle line), 25th percentile (bottom line of the box), and 75th percentile (top line of the box). The lowest and highest datum within 1.5 inter-quartile ranges for each category is represented by the ends of the whiskers. Median values of 'None', 'Few' and 'Many' with p-values were 3.8, 5.8, and 7.6 for ubiquitin particles (p=0.08), 3.6, 9.2, and 8.4 for KBH (p=0.02), and 3.8, 6.5, and 7.6(p=0.15) for KH.

Table 1

Distribution of Histologic Grades and Stages of the Study Population

Histologic features	Distribution (n=40)
Steatosis	
<5% (Grade 0)	0%
5–33% (Grade 1)	50.0%
34–66% (Grade 2)	27.5%
>66% (Grade 3)	22.5%
Lobular inflammation	
None	0%
<2 per 20X	72.5%
2–4 per 20X	22.5
>4 per 20X	5.0%
Portal inflammation	
None	5.0%
Mild	67.5%
More than mild	27.5%
Ballooning	
None	50.0%
Few	20.0%
Many	30.0%
Mallory-Denk bodies	
Absent/rare	77.5%
Many	22.5%
Fibrosis	
Brunt Stage 0	45.0%
Brunt Stage 1a,1b,1c	10.0%, 2.5%, 2.5%
Brunt Stage 2	15.0%
Brunt Stage 3	17.5%
Brunt Stage 4	7.5%
Steatohepatitis	
No	40.0%
Suspicious	20.0%
Definite	40.0%

Table 2

Zonal Distribution of KBH, Ub Particles, and KH

	KBH		Ub particles		KH	
	N	**percentage and 95%CI**	**N**	**percentage and 95%CI**	**N**	**percentage and 95%CI**
Zone 1	35	36.8% [27.8%, 46.9%]	495	34.4% [32.0%, 36.9%]	182	37.4% [33.2%, 41.8%]
Zone 2	5	5.3% [2.3%,11.7%]	1	0.1% [0.01%, 0.4%]	2	0.4%[0.1%, 1.5%]
Zone 3	55	57.9% [47.8, 67.3%]	941	65.5% [63.0%, 67.9%]	303	62.2% [57.8%, 66.4%]
Total	95	100%	1437	100%	487	100%

Abbreviations: N: numbers of the cells or ubiquitin particles; KBH, Keratin negative ballooned hepatocytes; Ub, ubiquitin; KH, Keratin negative normal size hepatocytes. Chi-square test for zonal distribution: KBH, $p<0.0001$; Ub particles, $p<0.0001$; KH, $p<0.0001$

Table 3

Relationship of KBH, Ub Particles, and KH to Fibrous Matrix in Different Zones

	KBH			Ub particles			KH		
	Total (N)	Adjacent to FM (N)	percentage of adjacent to FM and 95%CI	Total (N)	Adjacent to FM (N)	percentage of adjacent to FM and 95%CI	Total (N)	Adjacent to FM (N)	percentage of adjacent to FM and 95%CI
Zone 1	35	29	82.9% [67.3%, 91.9%]	495	493	99.6% [98.5%, 99.9%]	182	170	93.4% [88.8%, 96.2%]
Zone 2	5	5	100.0% [56.6%, 100%]	1	0	0%[−]	2	0	0%[−]
Zone 3	55	47	85.5% [73.8%, 92.4%]	941	856	91.0% [88.9%, 92.6%]	303	267	88.1% [84.0%, 91.3%]
Total	95	81	85.3% [76.8%, 91.0%]	1437	1349	93.9% [92.6%, 95.1%]	487	437	89.7% [86.7%, 92.1%]

Abbrev: N: numbers of the cells or ubiquitin particles; FM, fibrous matrix; KBH, Keratin negative ballooned hepatocytes; Ub, ubiquitin; KH, Keratin negative normal size hepatocytes. Chi-square test for association with FM and zonation of cells or particles: KBH, p=0.42; Ub particles, p<0.0001, KH, p=0.0016.

Table 4

Associations of KBH, Ub particles, and KH with histologic scores

Histologic features	KBH N/10 HPF	Ub particles N/10 HPF	KH N/10 HPF
Steatosis	(p=0.142)	(p=0.616)	(p=0.198)
5–33% (Grade 1)	2.0 ± 4.9	17.9 ± 41.7	6.6 ± 14.2
34–66% (Grade 2)	0.4 ± 0.8	18.9 ± 33.9	8.7 ± 11.3
>66% (Grade 3)	0.0 ± 0.0	3.6 ± 6.1	0.3 ± 0.8
Steatosis location	(p=0.001)	(p=0.005)	(p=0.0045)
Azonal	4.3 ± 6.8	55.5 ± 54.6	19.5 ± 16.2
Panacinar	0.0 ± 0.0	9.2 ± 18.7	4.2 ± 11.2
Zone 1	0.0 *	0.0 *	0.0 *
Zone 3	0.2 ± 0.7	0.7 ± 1.6	0.4 ± 0.8
Lobular inflammation	(p=0.05)	(p=0.008)	(p=0.259)
< 2 per 20X field	0.5 ± 1.6	9.8 ± 29.9	4.4 ± 10.2
2–4 per 20X field	3.5 ± 7.3	27.8 ± 46.5	8.6 ± 16.3
>4 per 20X field	0.0 ± 0.0	32.5 ± 33.8	14.9 ± 21.0
Portal inflammation	(p=0.16)	(p=0.028)	(p=0.083)
None	0.0 ± 0.0	0.0 ± 0.0	0.0 *
Minimal to mild	0.5 ± 1.2	9.4 ± 29.9	3.4 ± 9.4
More than mild	3.1 ± 6.7	31.4 ± 43.3	12.8 ± 16.3
Ballooning	(p=0.001)	(p<0.0001)	(p<0.0001)
None	0.02 ± 0.1	0.9 ± 3.9	0.08 ± 0.3
Few	0.4 ± 1.1	1.4 ± 2.2	0.9 ± 1.2
Many	3.3 ± 6.1	47.4 ± 50.4	18.7 ± 16.0
Mallory-Denk bodies	(p<0.0001)	(p<0.0001)	(p=0.0003)
Rare or Absent	0.1 ± 0.6	2.8 ± 10.5	1.4 ± 5.7
Many	4.4 ± 6.8	56.7 ± 53.4	19.5 ± 16.2
Fibrosis	(p=0.0002)	(p<0.0001)	(p=0.0032)
Brunt Stage 0	0.0 ± 0.0	0.4 ± 1.5	0.1 ± 0.6
Brunt Stage 1 (a, b, and c)	0.5 ± 1.3	0.5 ± 0.8	0.8 ± 1.2
Brunt Stage 2	0.2 ± 0.3	11.6 ± 22.2	5.2 ± 12.0
Brunt Stage 3	1.9 ± 2.0	48.7 ± 55.2	16.0 ± 12.3
Brunt Stage 4	9.2 ± 11.0	59.3 ± 57.0	26.5 ± 23.6
NAS score	(p=0.104)	(p=0.0003)	(p=0.024)
< 5	0.7 ± 1.7	8.9 ± 30.6	3.6 ± 9.9
≥ 5	2.2 ± 6.1	27.4 ± 39.7	11.2 ± 15.4
Steatohepatitis	(p=0.0036)	(p<0.0001)	(p=0.0001)

Histologic features	KBH N/10 HPF	Ub particles N/10 HPF	KH N/10 HPF
No	0.0 ± 0.0	0.0 ± 0.0	0.0 ± 0.0
Suspicious	0.5 ± 1.1	2.5 ± 6.1	0.4 ± 0.7
Definite	2.5 ± 5.4	36.1 ± 47.6	14.1 ± 15.7

Data are presented as the mean ± the standard deviation. P-values: Kruskal-Wallis test.

* N=1